Available online at www.sciencedirect.com
SCIENCE DIRECT®
PERGAMON
International Journal of Heat and Mass Transfer 46 (2003) 2857–2873
International Journal of HEAT and MASS TRANSFER
www.elsevier.com/locate/ijhmt

The onset of transient convection in bottom heated porous media

Ka-Kheng Tan *, Torng Sam, Hishamuddin Jamaludin

Department of Chemical and Environmental Engineering, University of Putra Malaysia, 43400 UPM, Serdang, Selangor, Malaysia

Received 27 May 2002; received in revised form 25 December 2002

Abstract

The theory of transient convection in bottom heated porous media under constant heat flux (CHF) condition or fixed surface temperature (FST) condition is advanced and verified by computational fluid dynamics (CFD) simulations. The use of κ^*, instead of κ_m tends to artificially inflate the value of Rayleigh number by about 30%. A new transient Rayleigh number for unsteady-state heat conduction was defined to predict the onset of transient convection in porous media, which were successfully simulated. The critical transient Rayleigh number from the simulation for CHF was about 29.60, which is close to the theoretical value of 27.1 calculated by Ribando and Torrance in 1976. In the case of FST, the critical transient Ra_c was found to be 30.9, which is close to the theoretical value of 32.3. The critical times of onset for simulations were predicted with good accuracy. The prediction of the critical wavelengths of the emerging plumes were fair for the 2D simulations. Any experiment to verify the linear stability analysis for thermal instability must simultaneously concur in the three eigenvalue parameters, namely the Biot number, the critical wavenumber and the corresponding critical Rayleigh number, apart from the physical boundaries. The average maximum transient Nusselt number was found to be 3.41 for CHF and 3.5 for FST respectively.

Keywords: Onset of convection; Transient Rayleigh number; Constant heat flux; Fixed surface temperature; Porous media

1. Introduction

Lord Rayleigh [1] first provided the famous instability criterion based on an adverse linear temperature gradient in a fluid layer. However in nature, natural convection is induced by a time-dependent and non-linear temperature profile. This means that the conventional steady-state linear stability analysis (LSA) is not applicable to convection caused by unsteady-state heat conduction. Several analyses and experiments had been done on the onset of convection caused by transient heat conduction in the past [34–36], none of them successfully developed an appropriate theory. Tan [2] and Tan and Thorpe [3–5] established a new theory of transient instability in deep fluids that successfully predicted the onset of convection under various boundary conditions.

The knowledge of natural convection in saturated porous media is of considerable interest because of its importance in the study of heat transfer of geothermal reservoir, mantle convection and various engineering applications, which include the high performance insulation for building, cold storage and solar power collection. Unsteady-state heat conduction experiments in porous media are very difficult to conduct as the measurement of the temperature profile of a non-homogeneous system cannot be done with certainty, let alone accuracy. Moreover, the heat conduction is not unidirectional and perpendicular to the interface. The computational fluid dynamics (CFD) simulations of onset of convection induced by unsteady-state heat conduction by Tan [1], Tan and Thorpe [4–6] and Sam [7] have successfully provided the mechanisms of onset and detailed temperature profiles and flow fields. In particular,

* Corresponding author. Tel.: +60-3-894-6284.
E-mail address: tankk@eng.upm.edu.my (K.-K. Tan).

0017-9310/03/$ - see front matter
doi:10.1016/S0017-9310(03)00045-0

Nomenclature

$\tilde{a}_c$	dimensionless wave number
a	wave number [m^{-1}]
b	gap between two walls of a Hele–Shaw cell [m]
c_p	specific heat [J/kg K]
d	diameter of beads [m]
g	acceleration due to gravity [m^2/s]
H	total depth of porous medium [m]
h	heat transfer coefficient [$W/m^2\,°C$]
h_s	heat transfer coefficient at surface from simulations [$W/m^2\,°C$]
K_e	permeability [m^2]
k	thermal conductivity of fluid [W/m °C]
k_m	thermal conductivity of porous media mixture, $k_m = \phi k_f + (1-\phi)k_s$ [W/m °C]
t_c	critical time for onset of convection [s]
T	temperature [°C]
T_s	surface temperature at time t [°C]
ΔT_c	critical temperature difference between top and bottom surface [°C]
ΔT_s	temperature difference of the surface of the porous media [°C]
w	width of the porous medium [m]
z	penetration depth [m]

Greek symbols

α	volumetric coefficient of thermal expansion [K^{-1}]
κ	thermal diffusivity [m^2/s]
κ^*	modified thermal diffusivity, $\kappa^* = k_m/(\rho c_p)_f$ [m^2/s]
κ_m	thermal diffusivity of porous mixture, $\kappa_m = k_m/\{\phi(\rho c_p) + (1-\phi)(\rho c_p)_s\}$ [m^2/s]
λ	wavelength [m]
v	kinematic viscosity [m^2/s]
μ	viscosity [Pa s]
ρ	density [kg/m^3]
ϕ	porosity

Abbreviation

CFD	computational fluid dynamics
CHF	constant heat flux
FST	fixed surface temperature boundary condition
LSA	linear stability analysis
Nu	Nusselt number

Subscripts

c	critical
0	initial condition
max	maximum
f	fluid
s	solid
m	porous media mixture

Sam's CFD simulations have shown that the onset of convection in porous media was basically similar to that in Newtonian liquids, although the detailed features may differ. Therefore it is useful to employ a CFD package to simulate the onset of convection in the porous media, the results were used to verify the theoretical value of critical transient Rayleigh number proposed in Section 3.

2. Literature review

This review will cover the LSA for porous media and for Hele–Shaw cell under steady-state heat conduction, followed by a review of the experiments for both steady-state and unsteady-state conditions. There are no known theoretical studies of the onset of convection in porous media caused by unsteady-state heat conduction.

2.1. Linear stability analysis for occurrence of convection in porous media

Horton and Roger [8] and Lapwood [9] were the early researchers who provided LSA to examine the breakdown of stability of a layer of fluid subject to an adverse temperature gradient in a porous media. Lapwood [9] pointed out that the problem was similar to the convection in a layer of viscous fluid, with the inclusion of Darcy's law.

The linear stability theory assumes an ideal linear temperature gradient in porous media, but the occurrence of convection under ideal steady-state condition could only be artificially achieved by gradually increasing the heating rate in a thin layer of porous medium over a long period of time. Usually an electrical heater was used to heat the surface. Under such condition it is highly doubtful that the fixed surface temperature (FST) boundary condition for bottom-heating, as claimed by most of the researches, would still be valid. Tan and Thorpe [3] had instead shown that these bottom-heating experiments are generally characterized by a constant heat flux (CHF) boundary condition, as the fluid on top of the conducting plate-heater will generate a Biot number close to zero. The latter was first used by Pearson [10] to conduct a LSA for Marangoni convection so as to correct Lord Rayleigh's (1916) misconception of Benard's [11] experiments that were thought to be driven by buoyancy. We have esti-

mated that the Biot number in most of the bottom-heating experiments using a plate heater could only be characterized by a CHF boundary condition as the fluid is rather insulating relative to the metal heater and typically a system of glass-water matrix heated by a copper heater will yield a Biot number of approximately 0.09.

Ribando and Torrance [12] were the first researchers to extend Lapwood's analysis to the case of bottom-heating with a CHF boundary condition and provided the theoretical values of critical Ra and $\tilde{a}_c$ as shown in Table 1. The CHF boundary condition may also exist for the upper boundary as in the case of top-cooling of a layer of porous media, although the theoretical values still have not been determined. They may be roughly estimated by comparing the results of Ribando and Torrance [12] with those for continuous fluids of Sparrow et al. [13] under the same boundary conditions.

Elder [14] re-arranged the thermal instability criterion of Horton and Roger [8] and Lapwood [9] in the form of Rayleigh number for porous media as $Ra = K_e g\alpha\Delta T H/(\kappa^* v)$, and for Hele–Shaw cell as $Ra = g\alpha\Delta T/(12bk_f v)$, both of which have theoretical value of $Ra_c = \pi^2$ and a critical wavenumber $\tilde{a}_c$ of π for rigid surfaces with the FST boundary condition. However, Elder did not mention the reason for employing the modified thermal diffusivity, $\kappa^* = k_m/(\rho c_p)_f$, in calculating the Rayleigh number, and clearly, he has mistaken the thermal boundary to be of the FST and the corresponding value of the critical Rayleigh number to be $4\pi^2$ and hence κ^* would give a higher value of Rayleigh number, whereas the correct definition of thermal diffusivity of the saturated porous media should be $\kappa_m = k_m/[\phi(c_p)_f + (1-\phi)(\rho c_p)_s]$. Neglecting the contribution of the solid, the calculation of κ^* can easily inflate its value by about 30% or more depending on the porosity and properties of the matrix. In fact, most of the researchers were not aware of the influence of Biot number on the value of the critical Ra, as we shall show later in this section.

2.2. Steady-state convection experiments

The recent study of Shattuck et al. [15] still referred to their bottom-heating experiments to the FST boundary condition and used the critical theoretical value of Rayleigh number of $4\pi^2$ to design and evaluate their experiments. They erroneously used $Ra_c = 4\pi^2$ to calculate a value of permeability that is 2.5 times that of their experimental value calculated from Ergun's relation [16]. This can be easily corrected with a theoretical Rayleigh number of about 27.1 for a CHF boundary condition and an actual κ_m with a porosity of 0.26 for his ordered media. The Biot number of the bottom-heating interface may be easily determined to be about 0.05 as the highly conducting ceramic heater (AIN) has a high conductivity of 133 W/m K. Their measured critical wavenumber of 0.7π is quite close to the theoretical value of 0.56π. However, the bulk fluid of the porous media exerts a substantial shear so that a free surface is not attainable in the presence of the solids. It is likely that the upper physical boundary is between that of a free and solid surface, hence the critical Ra will lie between 17.7 and 27.1, with an average of about 22.7. The corresponding critical wavenumber will thus be about 0.65π as an average of 0.56π and 0.73π. Tan and Thorpe [2] has also observed similar effect of laminar shear in bulk fluid in bottom-heating experiments using Newtonian fluids, the upper boundary in the bulk fluid experienced substantial laminar shear so that it is not free.

In general, past experiments were mostly based on the FST as isothermal and rigid conducting impermeable boundaries. Horton and Roger [8] conducted experiments to verify the theoretical result for the bottom-heating of porous media for the FST boundary condition using different grade of sand saturated with water. In their experiments, large temperature differences between the upper and lower boundaries were applied to generate the convective flow and non-linear temperature profile. As a result, the minimum temperature gradient, which they obtained from the experiment were in excess by considerable amounts of the minimum

Table 1
Criteria of thermal instability for porous media under various boundary conditions

Boundary conditions		Author	Wave number	Critical Rayleigh number
Top surface	Bottom surface			
FST, solid impermeable	FST, solid impermeable	Lapwood [9]	π	39.5
FST, free permeable	FST, solid impermeable	Lapwood [9]	0.67π	25.0[a]
FST, solid impermeable	CHF, solid impermeable	Ribando and Torrance [12]	0.73π	27.1
FST, free permeable	CHF, solid impermeable	Ribando and Torrance [12]	0.56π	17.7
CHF, solid impermeable	FST, solid impermeable	Estimated	0.73π	27.1
CHF, free permeable	FST, solid impermeable	Estimated	0.55π	14.0

[a] Lapwood [9] has found this value for a porous medium with water on top, i.e. for a CHF impermeable boundary, and he did not obtain results for a top free-surface per se. It should be around 25, which is close to 27.1.

temperature gradient that was predicted by the LSA theory. They claimed that this was possible because they neglected the temperature-dependence of viscosity, and consequently, they attempted to compare their experiments with theories and correlations, which allow for non-linear temperature profile and temperature-dependent viscosity. However they failed to propose a comprehensive solution. In fact, their experiments were already against the basis of the LSA due to the existence of a non-linear temperature profile, which may be due to the improper heating method and the large layer of porous media.

The homogeneous Darcian flow in a steady-state experiment is possible only when $d/H \ll 1$, which is not easy to meet in an experiment if large particles are favoured. Experiments of Georgiadis et al. [18] and Shattuck et al. [15] with 3.2-mm arylic spheres could only packed up to four layer thick, so that $d/H = 0.25$, which is not sufficiently small. This was the main cause of the deviation of experiments from theory.

The definition of thermal diffusivity for calculating the Rayleigh number in porous media had seen much confusion and disputes. Hortan and Roger [8] and Lapwood [9] had defined the Rayleigh number using the thermal diffusivity of the saturated porous media. However, Katto and Masuoka [17] suggested the use of κ^* for calculating Rayleigh number just because their experimental results for nitrogen gas agreed with the theoretical critical Rayleigh number of 39.4.

It is clear from our foregoing deliberation that the experiment is likely to be one of CHF and the critical *Ra* may be reduced to a low value of about 27.1 based on κ_m. In their experiments, high temperature of 40–80 °C and pressure of 50–100 atm have been used to induce the occurrence of convection in porous media. Their results were very doubtful as these extreme conditions may already violate the basis of the LSA theory.

Elder [14] investigated the onset of convection in both porous media and Hele–Shaw cell for bottom heating of FST boundary condition. In porous media, glass spheres of diameter 3, 5, 8, 18 mm and plastic balls of (styropor) 6 mm were used. However the critical temperature difference ΔT_c and the thickness of the porous layer and the type of fluid were not reported in his paper to afford a detailed analysis here. He claimed without determining the Biot number of the bottom interface that convection occurred at the theoretical value of $Ra_c = 4\pi^2$ which is doubtful as has been explained earlier. Kaneko et al. [19] used two different grades of silica sand of different permeabilities as porous media with heptane and ethanol as the saturated liquids. They found that for the system of heptane/sand B, the onset of convection occurred at Rayleigh number approximately $Ra_c = 4\pi^2$. However, the critical *Ra* for the ethanol/sand system was only 28, which is close to the theoretical value of 27.1 for CHF boundary. Chen and Chen [20] conducted experiments using 3-mm diameter glass beads contained in a box of $24 \times 12 \times 4$ cm^3. The average porosity was measured to be about 0.345. The occurrence of convection was marked by a change in the slope of the heat flux curve. They found a critical Rayleigh number of 40.07 with a critical $\Delta T_c = 15.2$ °C using κ^*. The inclusion of the solid and the porosity of 0.345 in κ_m would easily reduce the critical Rayleigh number by about 30% to a value that is close to 27.1 for a CHF boundary.

Overall, we may remark that most of these so-called FST experiments with bottom-heating are CHF type and their critical Rayleigh number can be easily reduced by 30% with κ_m to about 30, which is close to the theoretical value of 27.1.

2.3. Transient convection experiments

There have been no systematic studies on the onset of convection induced by transient heat conduction in deep layer of porous media. Elder [21] was the pioneer who conducted some numerical analyses and experiments on the onset of convection in porous media and Hele–Shaw cell. Owing to the difficulties in visualizing the convective flow in the porous media and the analogy between the hydrodynamic equations between the Hele–Shaw cell and porous media, Hele–Shaw cell was used in his experiments to gain qualitative information on the formation and development of the thermals, and the experimental results of Hele–Shaw cell were then compared to the numerical results of the porous media. He observed an array of blobs or plumes rapidly growing above the lower surface (proto-sublayer), then followed by the gradual appearance of a large-scale cellular pattern of ever changing eddies. Unfortunately, he was unable to develop a successful model for predicting the onset of transient convection.

Very recently, Prakash et al. [22] erroneously characterized their CFD study of the onset of convection in deep porous media with anomalously large Rayleigh number of 10^{10}, primarily because they wrongly defined the Rayleigh number with the full height of the box of 2 m. Some studies are focused on the post-onset and high Rayleigh number flows, for example Stamps et al. [23] conducted numerical study for unsteady convection at Rayleigh number exceeding 800.

The experiments for unsteady-state heat conduction in deep porous media [15,18] with $d/z_{max} = 0.17$ for 3 mm beads and $d/z_{max} = 0.46$ for 15 mm beads, the relatively short duration of transient experiments of few minutes compared to hours long steady-state experiments have very definite advantages of less fluctuations of experimental conditions and well-defined temperature profiles associated with the Biot number of the interface. Shattuck et al. [15] seemed to have obtained better results in their experiments with small temperature difference of less than 10 °C.

More interesting is the recent discovery of the rise of the plume by a team of Dutch scientists (as reviewed by Kerr, [24] sp.), instead of the conventional of convection rolls confined between two plates, from near the bottom of the mantle all the way up to Iceland's surface. The rising mantle plume is likely to be driven by the CHF mode of heating because the conductivity of the rocky mantle is only about a tenth of that of the outer core, which is composed mostly of iron. Anderson's [25] review showed that the thermal conductivity of the outer core (43 W/m K) is about 6.8 times that of the mantle (6.2 W/m K).

None of these researchers mentioned above have shown that their bottom-heating experiments had large enough Biot number and were FST, which has been shown by Tan and Thorpe [4] to be practically impossible; the experiments are, on the contrary, of the CHF boundary condition. It is conceivable that experiments for unsteady-state heat conduction in porous media are very difficult to conduct as the measurement of the temperature profile of an inhomogeneous system cannot be done with certainty. Moreover, the heat conduction is not uni-directional and not perpendicular to the interface.

It seems clear that the Rayleigh number can only be calculated accurately at a very strict condition where the thermal diffusivity of the solid and liquid matrix are similar and the permeability of the porous media should be large enough so that ΔT_s or heat flux will be small. In this study, a transient Rayleigh number based on Tan and Thorpe's [3] theory was proposed for a semi-infinite saturated porous medium heated with CHF or FST. A CFD package was used to simulate the onset of convection in the porous media in order to investigate the correctness of the theory and its prediction of the onset of convection.

3. Theory of onset of convection caused by transient heat conduction in porous media

The mathematical principle advanced by Tan and Thorpe [3–5] for predicting the onset of convection induced by transient heat conduction in semi-infinite fluid is adopted here for porous media.

The transient Rayleigh number for a porous media is a function of penetration depth z and the local temperature gradient $\partial T/\partial z$, thus a time-dependent Rayleigh number may be defined as:

$$Ra = \frac{K_e g \alpha z^2}{\kappa_m v}\left(\frac{\partial T}{\partial z}\right) \tag{1}$$

3.1. Constant heat flux boundary condition

When the bottom surface of a porous medium saturated with fluid is heated (or cooled) by a CHF, q^0, the temperature profile is predicted by Carslaw and Jaeger [26] as:

$$T_0 - T_s = \frac{2q^0\sqrt{\kappa_m t}}{k_m} ierfc\left(\frac{z}{2\sqrt{\kappa_m t}}\right) \tag{2}$$

By differentiating Eq. (2), the temperature gradient can be found as

$$\left(\frac{\partial T}{\partial z}\right)_t = -\frac{q^0}{k_m} erfc\left(\frac{z}{2\sqrt{\kappa_m t}}\right) \tag{3}$$

The transient Rayleigh number, defined in Eq. (1), becomes

$$Ra = \frac{K_e g \alpha z^2}{\kappa_m v}\frac{q^0}{k_m} erfc\left(\frac{z}{2\sqrt{\kappa_m t}}\right) \tag{4}$$

The maximum transient Rayleigh number at any instant can be found by differentiation of Eq. (4) as follows:

$$\left(\frac{\partial}{\partial z} Ra\right)_t = \frac{K_e q \alpha t_c q^0 z}{\kappa_m v k_m}\left[2erfc\frac{z}{2\sqrt{\kappa_m t}} - \frac{z}{\sqrt{\pi\kappa_m t}} e^{-\frac{z^2}{4\kappa_m t}}\right] = 0 \tag{5}$$

which gives the position of the maximum value of transient Ra as

$$z_{max} = 1.682\sqrt{\kappa_m t} \tag{6}$$

The maximum Rayleigh number at the onset of instability and subsequent convection may be expressed in terms of critical time t_c as:

$$Ra_{max} = \frac{0.6634 K_e g \alpha t_c q^0}{k_m v} \tag{7}$$

or in the conventional form.

$$Ra_{max} = \frac{K_e g \alpha \Delta T_s (0.587\sqrt{\kappa_m t_c})}{\kappa_m v} \tag{8}$$

The critical time at the onset of convection can be estimated with $Ra_{max} = 27.1$ as follows:

$$t_c = 2131\left(\frac{v\sqrt{\kappa_m}}{K_e g \alpha \Delta T_s}\right)^2 \quad \text{or} \quad \frac{40.9 k_m v}{K_e g \alpha q^0} \tag{9}$$

since ΔT_s can be substituted by Eq. (2).

The wavelength of the 3D convective plumes with a shape of the roll and $\tilde{a}_c = 2.3$ can be predicted as:

$$\lambda_c = \frac{2\pi z_{max}}{\tilde{a}_c} = 4.59\sqrt{\kappa_m t_c} \tag{10}$$

The wavelength of hemispherical plumes can be predicted from [5]:

$$\lambda_c = \frac{7.66 z_{max}}{\tilde{a}_c} = 5.60\sqrt{\kappa_m t_c} \tag{11}$$

The difference of sizes between the two shapes is 20% and may not be easy to distinguish in an experiment as

the plumes evolve from the thermal boundary layer. The plume will initially form a narrow filament and will reach a critical size of $5.6\sqrt{\kappa_m t_c}$ before detaching from the thermal boundary layer.

3.2. Fixed surface temperature boundary condition

When the surface of a porous medium saturated with fluid is heated (or cooled) by a step change in temperature instantaneously to a FST T_s, the temperature profile in the bulk fluid of temperature T_0 initially is predicted by Carslaw and Jaeger [26] as:

$$\frac{(T-T_s)}{(T_0-T_s)} = erf\left[\frac{z}{2\sqrt{\kappa_m t}}\right] \tag{12}$$

The temperature gradient can be found by differentiating Eq. (12)

$$\left(\frac{\delta T}{\delta z}\right)_t = -\frac{(T_0-T_s)}{\sqrt{\pi\kappa_m t}} e^{-\frac{z^2}{4\kappa_m t}} \tag{13}$$

The transient Rayleigh number as defined in Eq. (1) becomes

$$Ra = \frac{K_e g\alpha z^2}{\kappa_m \nu}\frac{(T_0-T_s)}{\sqrt{\pi\kappa_m t}} e^{-\frac{z^2}{4\kappa_m t}} \tag{14}$$

The maximum transient Rayleigh number at any instant can be found by differentiation of Eq. (14) as follows:

$$\left(\frac{\partial}{\partial z}Ra\right)_t = \frac{K_e g\alpha(T_0-T_s)}{\kappa_m \nu\sqrt{\pi\kappa_m t}} e^{-\frac{z^2}{4\kappa_m t}}\left[-\frac{z}{2\kappa_m t}\right] = 0 \tag{15}$$

which gives the position of the maximum value of transient Ra as

$$z_{max} = 2\sqrt{\kappa_m t} \tag{16}$$

The maximum Rayleigh number at the onset of convection may be expressed in terms of critical time t_c as:

$$Ra_{max} = \frac{0.83K_e g\alpha(T_0-T_s)}{\nu}\sqrt{\frac{t_c}{\kappa_m}} \tag{17}$$

or in the conventional form with $\Delta T_c = (T_0 - T_s)$.

$$Ra_{max} = \frac{K_e g\alpha\Delta T_c(0.83\sqrt{\kappa_m t_c})}{\kappa_m \nu} \tag{18}$$

For a porous medium that is bounded by two solid surfaces, $Ra_{max} = \sqrt{4\pi^2}$, the critical time at the onset of convection can thus be estimated as follows:

$$t_c = 2262\left(\frac{\nu\sqrt{\kappa_m}}{K_e g\alpha\Delta T_c}\right)^2 \tag{19}$$

The critical wavelength for a convective cell with a shape of roll and $\tilde{a}_c = \pi$ can be predicted as:

$$\lambda_c = \frac{2\pi z_{max}}{\tilde{a}_c} = 4\sqrt{\kappa_m t_c} \tag{20}$$

when the shape of the plume is hemispherical, then the critical wavelength can be predicted from:

$$\lambda_c = \frac{7.66 z_{max}}{\tilde{a}_c} = 4.88\sqrt{\kappa_m t_c} \tag{21}$$

which is about 20% more than that for a roll.

4. Computational fluid dynamics simulations

A commercial CFD package, FLUENT, was used for the 2D time-dependent simulations for a homogeneous isotropic porous layer saturated with water under CHF or FST boundary condition and bounded by two rigid impermeable boundaries. The vertical walls were adiabatic. The top rigid surface was held at an initial temperature, $T_0 = 20$ °C. At time $t = 0$ s, the CHF boundary condition is attained by suddenly heating the bottom surface with a CHF, whereas the FST boundary condition surface was suddenly heated and maintained at a fixed temperature T_s.

FLUENT defined the porous media model with the input of permeability, porosity and the thermal properties of the solid and the liquid. The physical properties of the porous medium employed in this study were based on those of glass beads and water as shown in Table 2.

The permeability of porous media made of various sizes of glass beads were calculated from the Kozeny–Carmen relation [27].

$$K_e = \frac{d^2}{172.8}\frac{\phi^3}{(1-\phi)^2} \tag{22}$$

where d is the diameter of the glass beads and ϕ the porosity. Eq. (22) is similar to Ergun's relation [16] except that the coefficient of the denominator is 150 instead of 172.8.

Table 2
Physical properties of porous media at 20 °C

Properties	Glass beads	Water	Porous medium
Porosity (3-mm diameter beads)	–	–	0.345
Permeability (m^2)	–	–	4.99×10^{-9}
Density (kg/m^3)	2500	971	2225
Thermal conductivity (W/(m K))	1.14	0.613	0.956
Specific heat capacity (J/(kg K))	750	4180	835
Thermal diffusivity, κ_m (m^2/s)	7.05×10^{-7}	1.51×10^{-7}	3.16×10^{-7}

4.1. Size of domain and computation cell

The choice of the domain and computation cell is vital, as it will affect the natural development of the temperature profile and the formation of the plume. For the time-dependent simulation, the critical thermal depth and wavelength predicted by Eqs. (6) and (10) can be used to determine the computation domain and cell size with the known critical time from Eq. (9).

The thickness and width of the porous layer is set at a depth of $H \geqslant 3z_{\max}$ and a width of $w \geqslant 2\lambda_c$ in these simulation to approximate the semi-infinite fluid, so that there is ample space for the thermal plume to penetrate the bulk fluid unimpeded. In addition, the effect of aspect ratio has to be taken into account in determining the cell size. A general rule of thumb to avoid excessive ratio is $w/H \leqslant 5$. Excessive aspect ratio can lead to stability problem, convergence difficulties and propagation of numerical errors. The spacing between a wall and the adjacent grid line can reduce the accuracy of the computed sheer stress and heat transfer coefficient at the wall. The guidelines for the choice of the wall grid spacing in laminar flows was derived based on the analytical solution for fully-developed laminar flow plates separated by a height H as $\Delta n/H < 0.05$, where Δn is the size of computational cells.

5. Results of simulation for CHF and discussion

The results of simulations will be used to verify the theory set forth in Section 3, particularly the values of transient Rayleigh number, critical times and critical wavelengths. There exists no experimental data for the verification of the theory.

5.1. The formation and development of the thermal plumes

The development of the thermal boundary layer until the onset of instability and convection, and the formation of plumes induced by a CHF is similar to Elder's [28] observations as shown in Figs. 1–3. It can be characterized by three distinct regimes, namely,

(i) a quasi-stable regime in which a thermal boundary layer began to form and thickening but no fluid motion is observed. This is the conduction phase, Fig. 1.
(ii) a regime of very slow flow in which the velocity of the fluid started to accelerate in the localized unstable points. The thermal boundary layer became distorted and marked the onset of instability and the ensuing convection, Fig. 2.
(iii) the post-onset unstable regime in which the distorted thermal boundary layer extended and formed an array of growing plumes, Fig. 3. Occasionally the growing plumes may coalesce with neighboring plumes, which extended and detached and the next cycle began again.

The shape of the plumes for the porous media is finger-like, quite different from the hemispherical cap observed for plumes in continuous fluid. The rapid coalescence of evolving plumes rendered the observation and measurement of the plumes quite difficult.

5.2. Critical times and transient Rayleigh numbers

The onset of convection can be detected by the sudden increase in the fluid velocity and simultaneous change in heat transfer coefficient. FLUENT only recorded the minimum and maximum velocities, and the

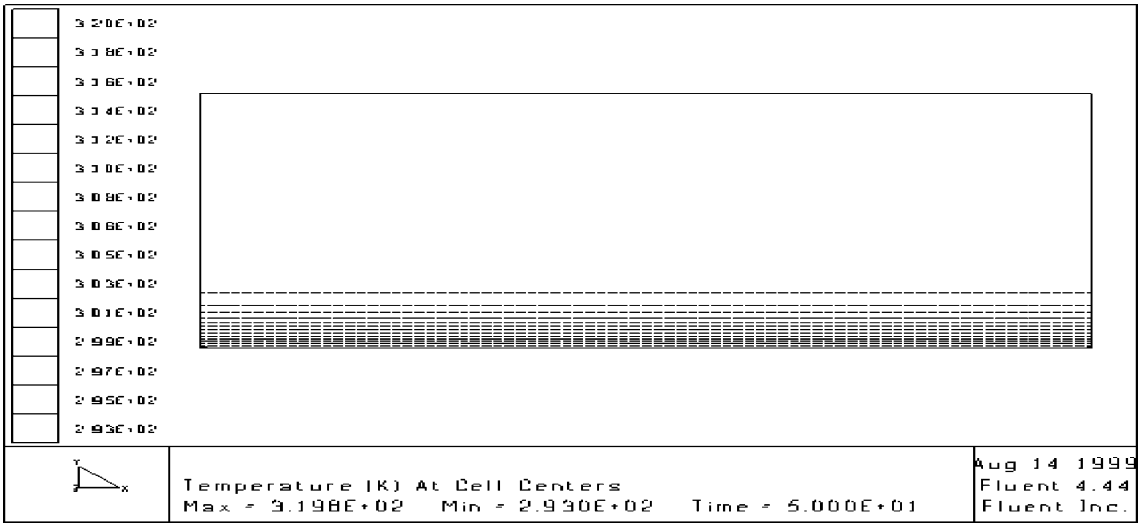

Fig. 1. Temperature contour of a porous medium of 3 mm glass beads saturated with water. CHF $q^0 = 5000$ W/m^2 at $t = 50$ s.

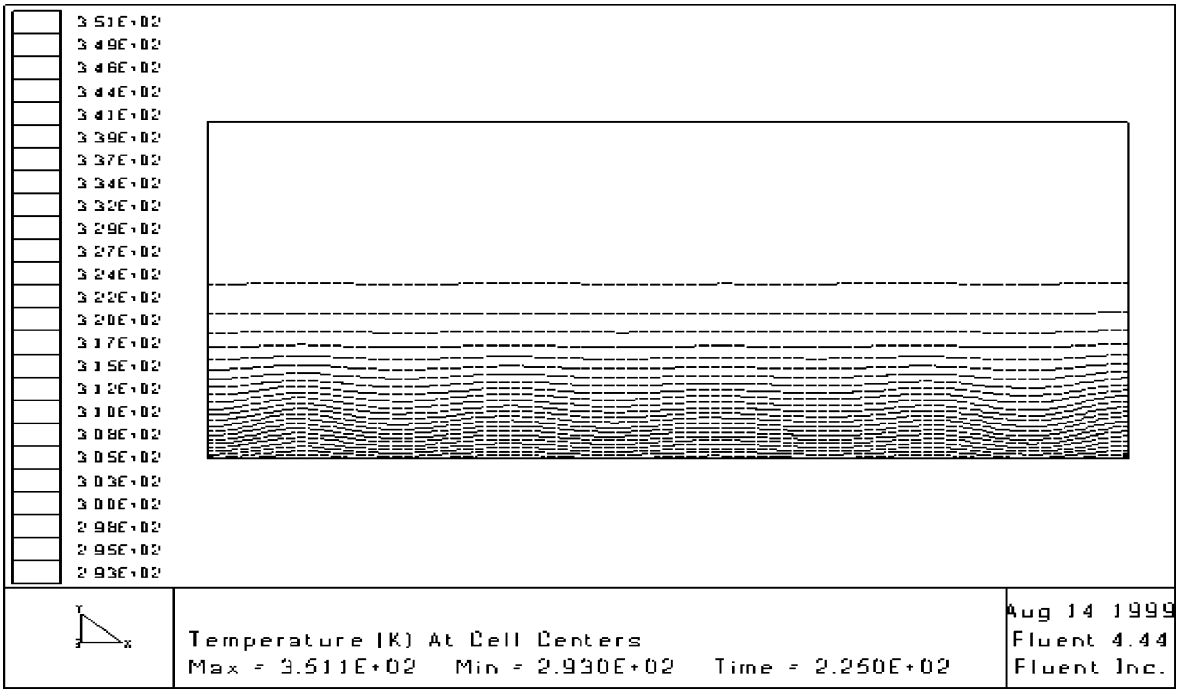

Fig. 2. The onset of instability in porous medium of 3 mm glass beads saturated with water. CHF $q^0 = 5000$ W/m^2 at time 225 s.

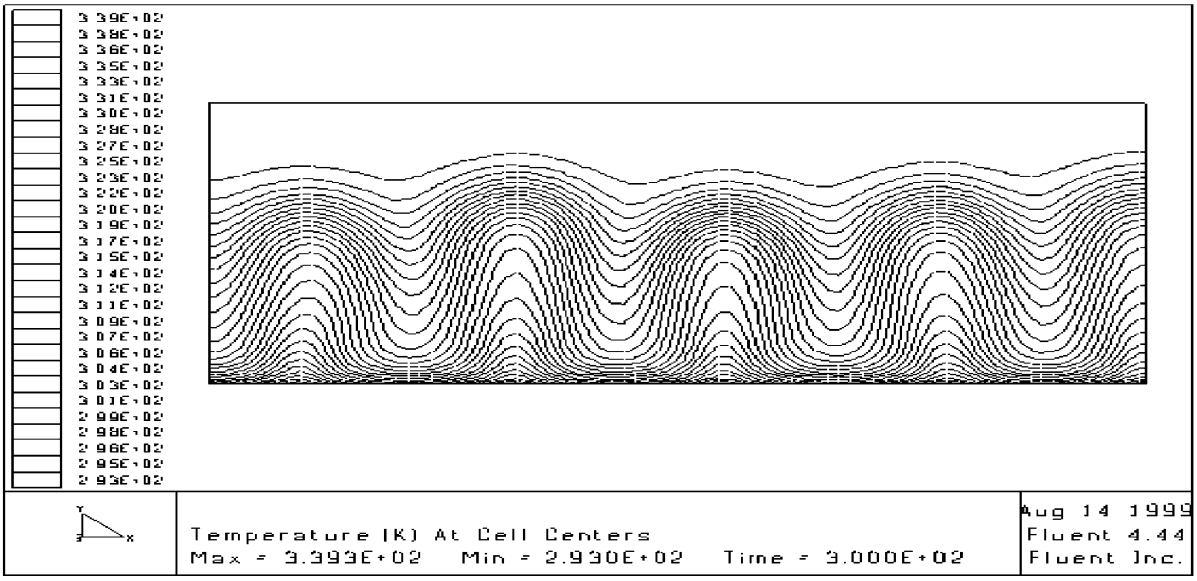

Fig. 3. The formation of plumes in porous medium of 3 mm glass beads saturated with water. CHF bottom heating at $q^0 = 5000$ W/m^2 at $t = 300$ s.

maximum velocity may be used to determine the onset of convection as shown in Fig. 4. It was found in the simulations that the maximum magnitude of velocity increased exponentially with time after the onset of instability. The fluid flowed upward rapidly in thin filaments and extended to form finger-like plumes. The convection phase was thus characterized by the formation and detachment of plumes. The range of the velocity at the onset of convection was found to be between 10^{-5} and 10^{-4} m/s depending on the rate of

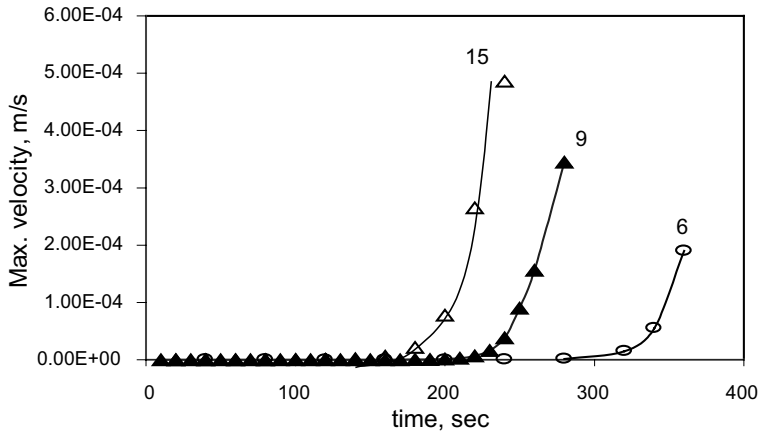

Fig. 4. Maximum velocities of water from various simulations for bottom heating with CHF boundary condition.

heating, although these microvelocities are only indicative of probable movement of only the fluid and not the glass beads. They are in the same order of magnitude of velocities measured by Horton and Roger [8], who observed the occurrence of convection through the wall of the glass container by means of a microscope, which tracked the movement of a layer of soluble dye in the medium. The initial motion occurred abruptly at a slow rate of about 1×10^{-5} m/s, while the velocity of the stationary liquid was less than 1×10^{-7} m/s. Therefore the maximum velocities calculated by the simulations are quite realistic.

The critical times are predicted by Eq. (9) with properties of the mean temperature of that of the heated surface and that of the bulk fluid. They are found to be in good agreement with those summarized in Table 3. Better predictions are obtained at small heat fluxes or small temperature differences, for example at 180 W/m^2 K for 15 mm diameter beads. The relatively bigger interstitial spaces between large spherical particles also allows more fluid to be present and respond more readily to the temperature disturbance. This is expected as the change of physical properties of the fluid at small change of temperature is not significant, while the effect of buoyancy is sufficiently discernable. The low critical Ra of CHF boundary predicts relatively short t_c compared to that of the FST boundary condition, this is the key feature of onset of instability at an insulating interface. The short critical time of CHF heating will generate more plumes per unit area since λ is proportional to the $\sqrt{t_c}$.

Table 3
Critical times from simulations and prediction for bottom heating of CHF boundary condition

Beads diameter (mm)	Heat flux (W/m^2)	ΔT_c (°C)	Critical times (s)	
			Simulation	Prediction based on κ_m
3	5000	58.1	225	196
	3500	49.4	340	310
6	2500	25.9	185	170
	3000	28.3	150	136
9	1200	14.2	240	216
	2000	17.4	130	115
15	500	5.1	180	237
	180	3.8	720	703

The critical transient Rayleigh numbers are calculated from the known heat fluxes and critical times observed in the simulations, as are shown in Table 4. The transient Rayleigh numbers are found to be independent of the critical times, and therefore also independent of the heat fluxes, as shown in Fig. 5. Thus the onset of instability and convection is a localized process confined within the thin thermal boundary layer. The average maximum transient Rayleigh number based on κ_m and Eq. (7) is 29.60, which is close to the theoretical value of 27.1 predicted by Ribando and Torrance [12], with a difference of only 10%. Indeed the closest value of 27.8 was obtained with the lowest ΔT_c of 3.8 °C for the 15-mm beads. The maximum transient Rayleigh number based on Eqs. (7) and (8) are as expected of small difference. However, the average Ra_c based on κ^* is 37.59, which is 39% higher than the theoretical value of 27.1. It is clear from our explanation in Section 2 that κ_m yields a more accurate prediction of Ra than those predicted by κ^*. This study also shows that transient convection induced by the unsteady-state heat conduction provides a better prediction of the critical Rayleigh number because the correct temperature profile for the boundary condition and the corresponding definition of Ra must be used for the prediction, i.e. for Bi = 0.

Table 4
Critical Rayleigh numbers from simulations for bottom heating of CHF boundary condition

Beads diameter (mm)	Heat flux (W/m^2)	ΔT_c (°C)	Critical Rayleigh number		
			Ra_c Eq. (7)	Ra_c Eq. (8)	Ra_c[a] Eq. (8)
3	5000	58.1	34.38	35.27	44.08
	3500	49.4	30.72	31.11	38.90
6	2500	25.9	29.52	29.69	37.16
	3000	28.3	31.32	31.87	39.88
9	1200	14.2	31.98	32.21	40.33
	2000	17.4	30.59	30.79	38.55
15	500	5.1	20.55	20.58	25.78
	180	3.8	27.75	28.75	36.02
Average			29.60	30.04	37.59

[a] Rayleigh number using thermal diffusivity $\kappa^* = k_m/(\rho c_p)_f$.

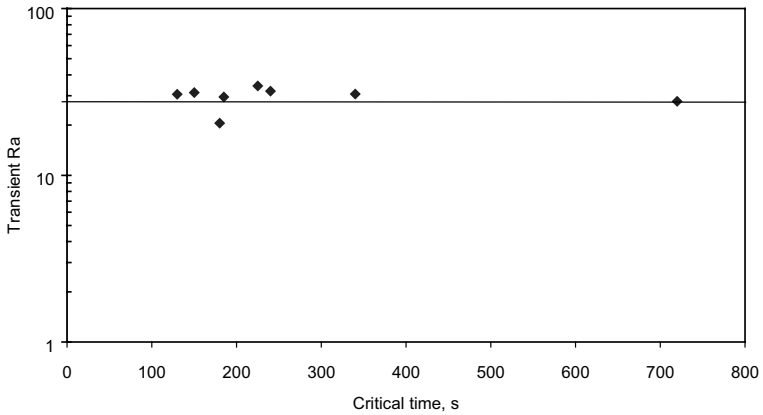

Fig. 5. Transient Rayleigh numbers from simulations for various porous media.

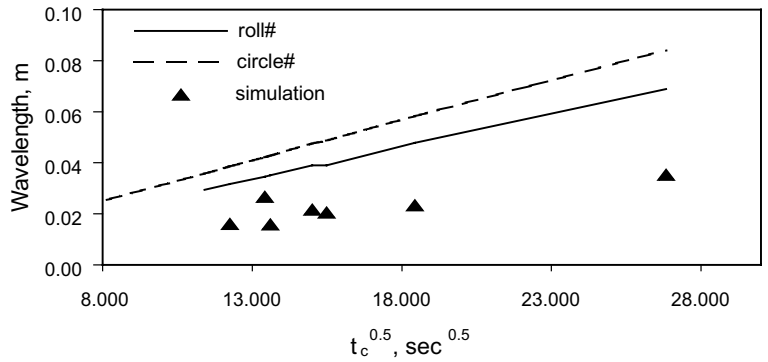

Fig. 6. Comparison of the critical wavelengths from simulations and the theory for bottom-heating of CHF boundary condition.

5.3. Critical wavelengths

The critical wavelengths or the sizes of the plumes were obtained by measuring the distance between two peaks of the plumes in simulations. They were found to agree fairly well with the prediction of Eqs. (10) and (11) as shown in Fig. 6. Strictly, the prediction of the sizes of 2D rolls can only be used to compare with the sizes of

plumes from 2D CFD simulations in this study. Tan's CFD [29] simulations with 2D and 3D models showed that the plumes in 3D simulations are more realistic compared to those observed in experiments. It is expected that 3D simulations will show that the actual 3D plumes will agree better with the prediction for hemispherical plumes. Hence 3D simulations should be conducted to study the development of the plume structure in porous media as both type of convective cell had been reported by Horne [30], Straus and Schubert [31], Chen and Chen [20], Lister [32] in their laboratory and numerical studies respectively.

5.4. Heat transfer and Nusselt number

The transient heat transfer coefficient from the simulation is found to increase suddenly at the onset of convection after an initial decrease in the conduction phase, Fig. 7. The critical time of about 200 s for the simulation of 6 mm beads has been predicted accurately by Eq. (9). Interestingly, the heat transfer coefficient for the conduction phase in the simulation lies between those predicted by k^* and k_m. The temperature profiles and heat flows are very accurately simulated by CFD. The gap may be narrowed by using the physical properties at each temperature that was altered by the ongoing unsteady-state heat conduction.

The transient Nusselt number is calculated by dividing the heat flux obtained from simulation by the heat flux by theoretical conduction [26], i.e. $Nu = q''_s/q''_c$, where $q''_s = h_s \Delta T_c$ from simulation and $q''_c = k_m \Delta T \sqrt{\pi/4\kappa_m t_c}$, i.e. $h_c = k_m \sqrt{\pi/(4k_m t_c)}$. The maximum transient Nusselt number is found to increase with the rate of heating, Table 5. The average value of Nusselt number calculated using κ_m is about 3.41, which is close to the theoretical value of 3 for steady-state convection calculated by Busse and Joseph [33] for $Ra = Ra_c$. Generally Nusselt numbers based on κ_m are 25% more than those calculated using κ^*, Fig. 8. However, we note that the actual Nu will be appreciably higher than those of the present 2D model. Indeed Tan's [29] 3D time-dependent simulation for liquids shows that Nu for 3D simulations may be about 30% higher than those of 2D. This may be due to higher surface area of a 3D plume than that of a 2D roll. The average Nusselt for the whole cycle is roughly 2.

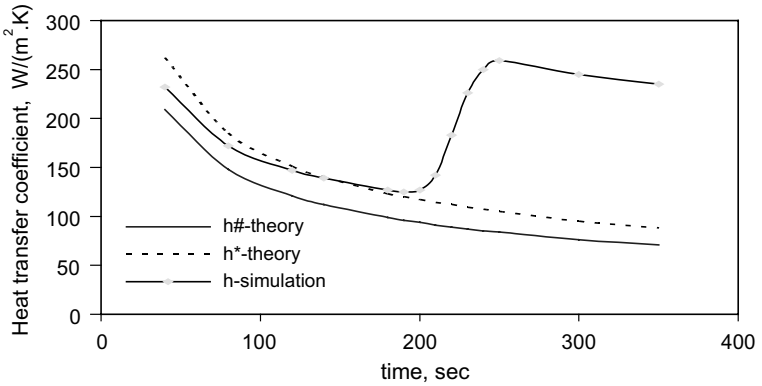

Fig. 7. Heat transfer coefficient at various times for bottom-heating, $q^0 = 2500$ W/m^2 at $t_c = 185$ s for 6-mm glass beads.

Table 5
Maximum Nusselt number from simulations for bottom-heating of CHF boundary condition

Run no.	Beads size (mm)	Heat flux, q^0 (W/m^2)	Domain size (cm)	Boundary condition CHF	
				Nu^a	Nu^b
3	6	2500	3×4	3.30	2.60
4	6	3000	3×4	3.75	3.00
6	9	2000	4×5	3.05	2.43
7	15	500	3×4	3.55	2.85
Average				3.41	2.72

[a] Nusselt number calculated using κ_m.
[b] Nusselt number using κ^*.

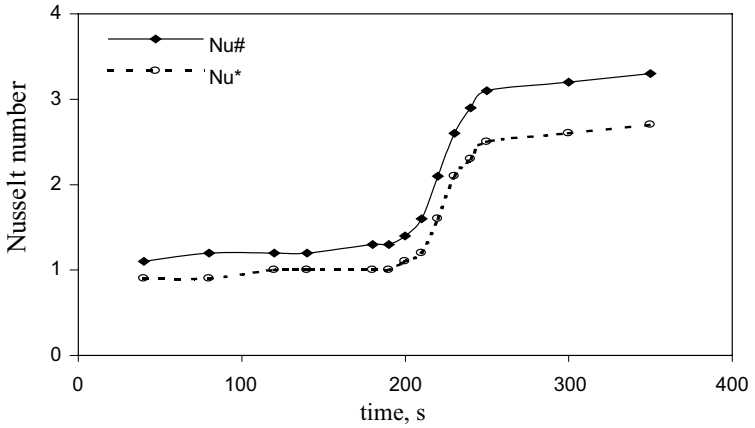

Fig. 8. Nusselt number for bottom-heating of CHF, $q^0 = 2500$ W/m^2 for 6-mm glass beads.

6. Results of simulation for FST and discussion

6.1. Critical transient Rayleigh numbers and critical times

The critical transient Rayleigh numbers were calculated from properties of the mean temperature of the porous media and the critical times from the simulations. The average maximum transient Rayleigh numbers was found to be 30.9 and 38.7 based on κ_m and κ^* respectively from Eq. (18). The one based on κ^* is the correct value as it is close to the theoretical value of 39.5 predicted by Lapwood [9]. However the properties based on κ^* is unrealistic as it does not take account of the contribution from those of the solids, and it tends to inflate the value of the Rayleigh number. It is important to note that transient convection originated in the thermal boundary layer in deep fluids is restrained by a upper boundary that is provided by a laminar shear layer, which is not a free surface characterized by $du/dy = 0$. Therefore, the critical Rayleigh number will lie between that of a upper free and upper solid surface, that is between 25.0 and 39.5 as shown in Table 6, the value is 32.3. The simulated average transient Rayleigh number of 30.9 based on κ_m is thus very close to the theoretical value of 32.3.

The simulated critical times are found to be in good agreement with those predicted by Eq. (19) with a critical Rayleigh number of 32.3. Indeed, the penetration depth, $z_p = 2\sqrt{\kappa t}$, for 40 s, 9.1 mm in a porous medium, smaller than the beads diameter (15 mm). The effect of lateral heat transfer may not be as in cases of small beads (Figs. 9–12).

Table 6
Critical times and transient Rayleigh numbers from simulations

Beads diameter (mm)	ΔT_s (°C)	Critical times (s)		Critical Rayleigh number	
		Simulated	Predicted	Ra_c[a]	Ra_c[b]
3	45	225	253	30.46	38.09
	30	900	1000	30.63	38.33
6	15	450	550	29.20	36.56
	20	180	219	29.27	36.65
9	30	15	12	35.59	44.53
	20	40	42	31.14	38.98
15	5	180	220	28.53	35.73
	10	40	39.5	32.38	40.55
Average				30.90	38.68

[a] Rayleigh number is calculated by using thermal diffusivity $\kappa_m^{\#} = k_m/[\phi(\rho c_p)_f + (1-\phi)(\rho c_p)_s]$.
[b] Rayleigh number by $\kappa^* = k_m/(\rho c_p)_f$.

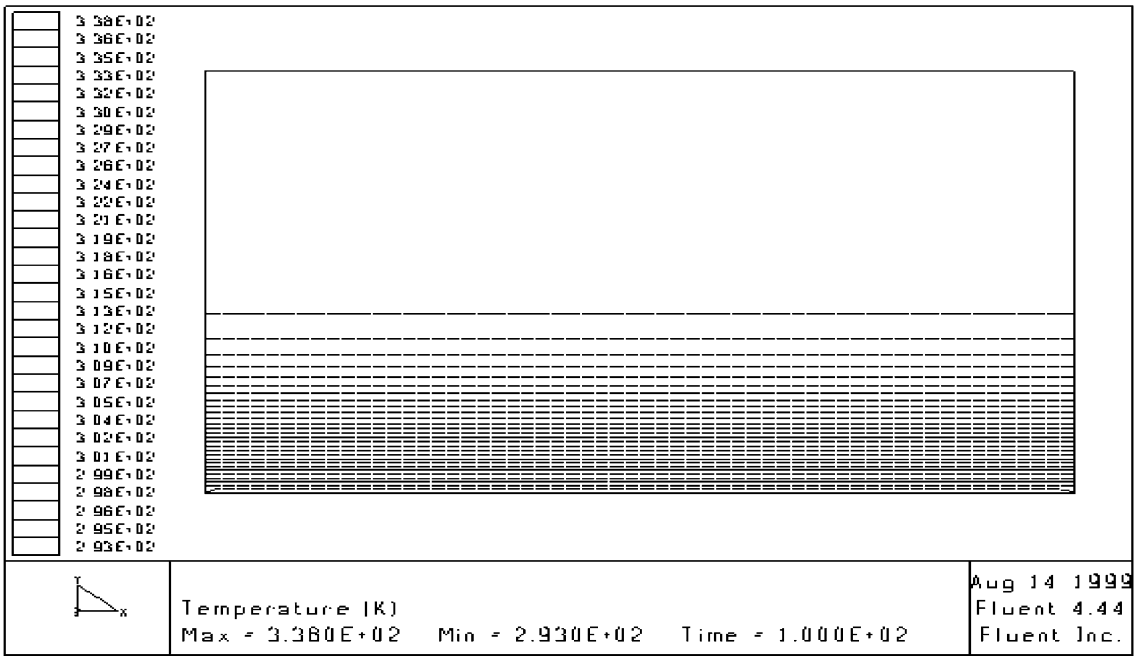

Fig. 9. Temperature contour for 3 mm glass beads saturated with water. FST bottom heating at $\Delta T_s = 45$ °C at $t = 100$ s.

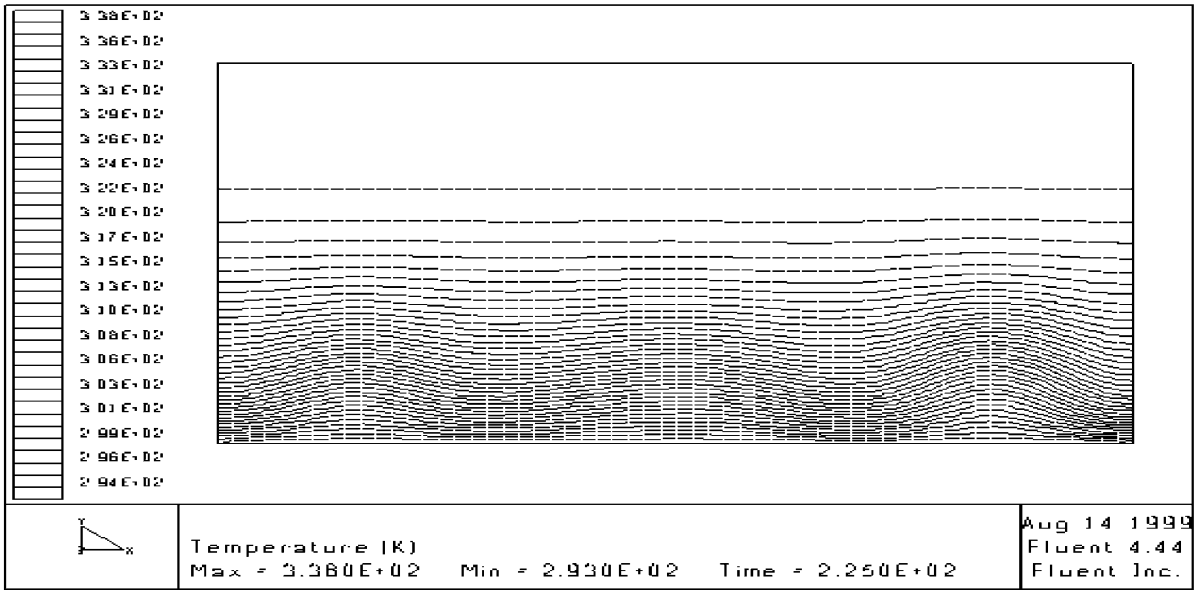

Fig. 10. The onset of instability and convection for 3 mm glass beads saturated with water. FST bottom heating at $\Delta T_s = 45$ °C at $t_c = 225$ s.

6.2. Critical wavelengths

The critical wavelengths or sizes of the plumes were found to agree fairly well with the 2D prediction of Eqs. (20) and (21) as shown in Fig. 13. It is expected that 3D plumes will agree better with the prediction for hemispherical plumes.

6.3. Heat transfer and Nusselt number

The heat flux from simulation is seen to increase abruptly and rapidly after the onset of convection at about 50 s for 15-mm beads, Fig. 14. The initial conduction phase has been simulated very well up to the point of onset of instability at 40 s, which has been predicted by Eq. (19).

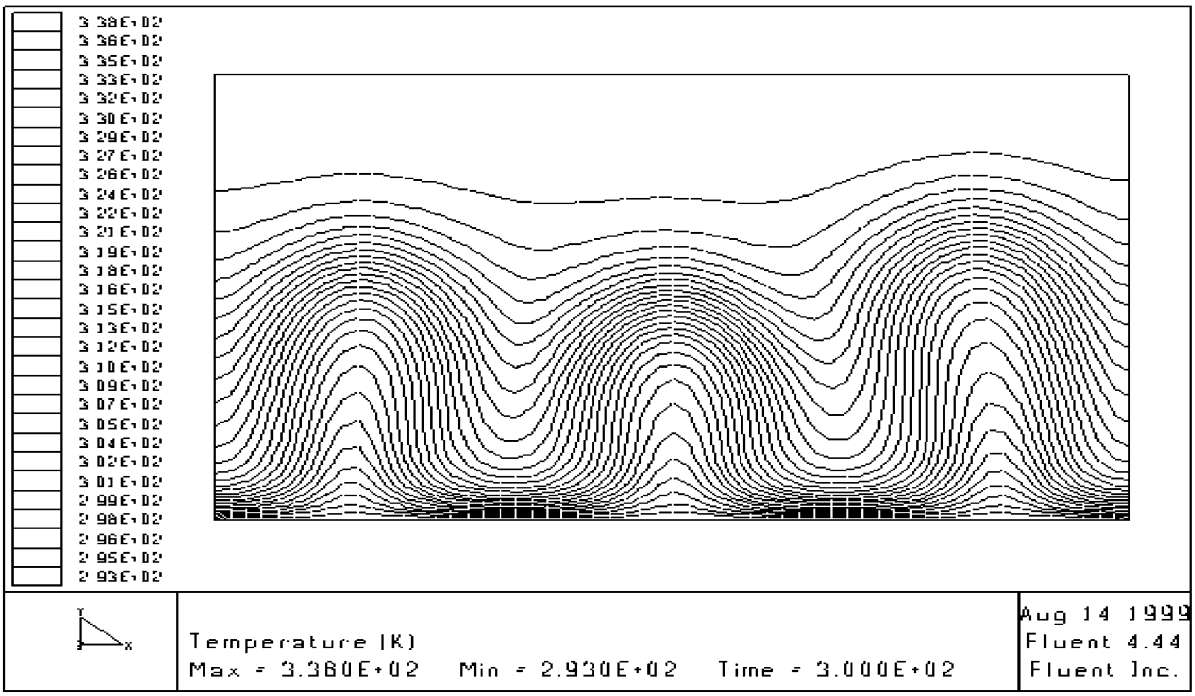

Fig. 11. Formation of finger-like plumes for 3 mm glass beads saturated with water. FST bottom heating at $\Delta T_s = 45$ °C at $t = 300$ s.

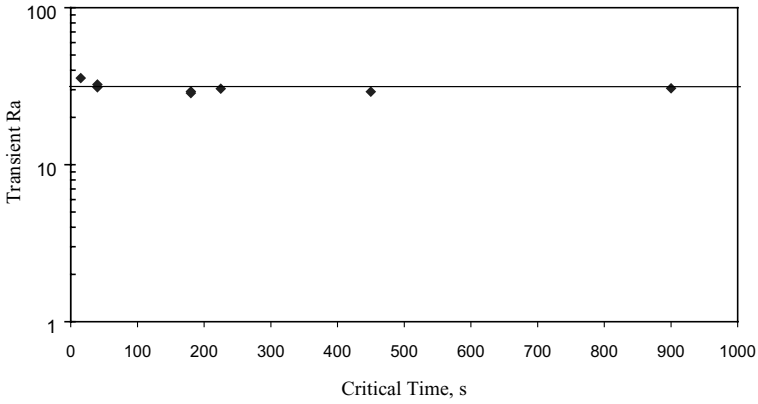

Fig. 12. Transient Rayleigh numbers from simulations for various porous media.

The Nusselt number defined as the ratio of the actual heat flux by convection to the heat flux by theoretical heat conduction is equal to 1 before the onset of convection. The transient Nusselt number calculated by dividing the simulated heat flux obtained by the heat flux of theoretical heat conduction at each instant (24), i.e. $Nu = q''_s/q''_c$, is found to increase rapidly after the onset of convection until a maximum value of about 3.5, Fig. 15. The average value of 3.46 is a good estimate of the actual 3D heat transfer process (27). The transient Nusselt numbers calculated using κ_m are about 25% more than those based on κ^* (Table 7). The development of the thermal boundary layer until the onset of convection induced by the FST boundary condition is similar to that of the CHF boundary as shown in Figs. 9–11.

7. Conclusions

It was found that most bottom-heating experiments are characterized by an insulating CHF boundary condition, hence the Biot number of the bottom interface should be zero, and its corresponding critical Rayleigh

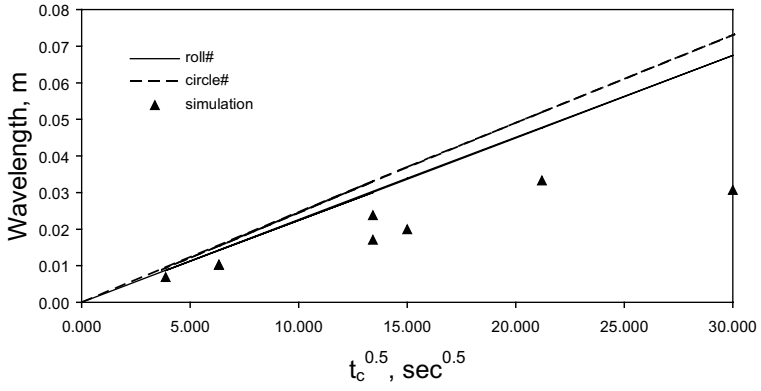

Fig. 13. Comparison of the critical wavelengths from simulations and the theory for bottom-heating of FST boundary condition.

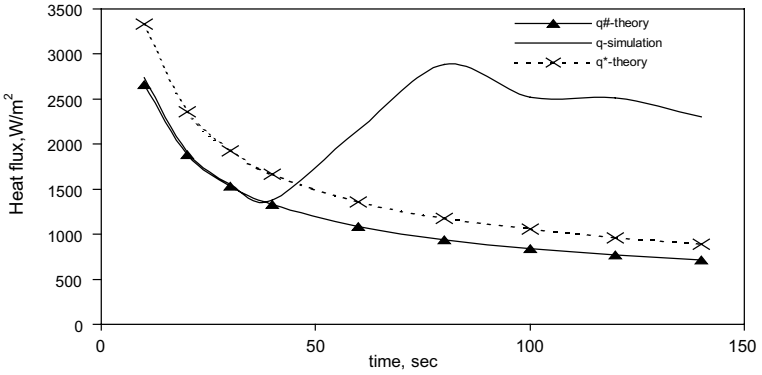

Fig. 14. Heat flux at various times for FST boundary condition (15-mm glass beads, $\Delta T_s = 10$ °C, at $t = 50$ s).

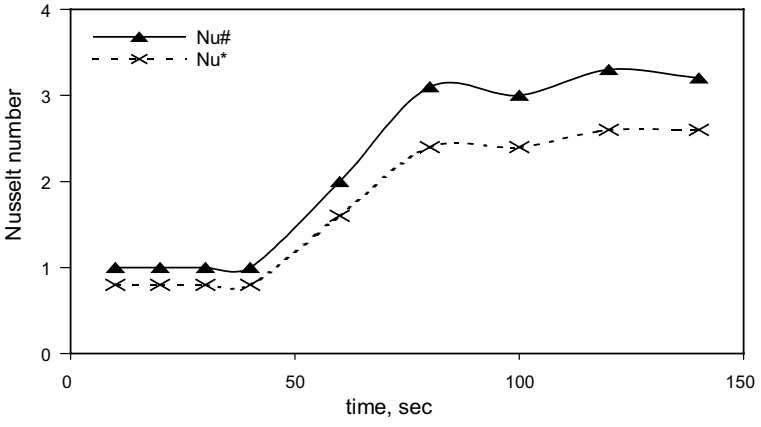

Fig. 15. Rapid increase of Nusselt number over time (for 15-mm glass beads, $\Delta T_s = 10$ °C, at $t = 50$ s).

number should be 27.1, instead of 39.5 assumed for a conducting boundary.

The onset of convection induced by unsteady-state heat conduction in porous media under CHF boundary condition has been successfully simulated using FLUENT. The formation and development of the thermal plume can be divided into three regimes, namely the conduction regime, the onset of instability or convection

Table 7
Maximum Nusselt number from simulations for bottom heating of FST boundary condition

Beads diameter (mm)	Domain size (cm)	ΔT_s (°C)	Critical times (s)	Nusselt numbers	
				Nu^a	Nu^b
6	3×5	15	450	3.10	2.48
9	3×5	20	40	3.45	2.75
9	4×6	30	15	4.15	3.32
15	3×4	10	40	3.15	2.50
Average				3.46	2.76

[a] Nusselt number calculated using κ_m.
[b] Nusselt number using κ^*.

and the post-convection regime. The simulated critical transient Rayleigh number based on κ_m is close to the theoretical value of 27.1. The critical times can be predicted accurately with our theory and the predictions of critical wavelengths were fair.

The maximum transient Nusselt number based on κ_m is in the range of 3.3–3.8.

The onset of convection in porous media induced by unsteady state heat conduction for FST boundary condition has been successfully simulated using a CFD package. The simulated critical transient Rayleigh number has been found to be in good agreement with the theoretical value of 32.3 from LSA. The critical times for the onset of instability and convection have been predicted accurately.

The maximum transient Nusselt numbers based on $\kappa^{\#}$ from simulations was in the range of 3.1 to 4.15, with an average of 3.46.

References

[1] R. Lord, On convective currents in a horizontal layer of fluid when the higher temperature is on the under side, Phil. Mag. 32 (1916) 529.
[2] K.K. Tan, Gas Diffusion into viscous and non-newtonian liquids and the onset of convection, PhD Dissertation, Department of Chemical Engineering, University of Cambridge, 1994.
[3] K.K. Tan, R.B. Thorpe, The onset of convection caused by buoyancy during transient heat conduction in deep fluids, Chem. Eng. Sci. 51 (1996) 4127–4136.
[4] K.K. Tan, R.B. Thorpe, The onset of convection driven by buoyancy effects caused by various modes of transient heat conduction. Part 1: Transient Rayleigh numbers, Chem. Eng. Sci. 54 (1999) 225–238.
[5] K.K. Tan, R.B. Thorpe, The onset of convection driven by buoyancy effects caused by various modes of transient heat conduction. Part II: The sizes of plumes, Chem. Eng. Sci. 54 (1999) 239–244.
[6] K.K. Tan, R.B. Thorpe, On convection driven by surface tension caused by transient heat conduction, Chem. Eng. Sci. 54 (1999) 775–783.
[7] T. Sam, Simulations of the onset of convection in porous media induced by unsteady-state heat conduction, M.Sc. thesis, University Putra Malaysia, 1999.
[8] C.W. Horton, F.T. Rogers Jr., Convection current in a porous medium II. Observation of condition at onset of convection, J. Appl. Phys. 20 (1949) 1027–1029.
[9] E.R. Lapwood, Convection of a fluid in a porous medium, J. Fluid Mech. 44 (1948) 508–521.
[10] J.R.A. Pearson, On convection cell induced by surface tension, J. Fluid Mech. 19 (1958) 341.
[11] H. Benard, Lees tourbillons cellulaires dan une nappe liquide trasportant de la chaleur par convection en regime permanent, Ann. Chem. Phys. 23 (7) (1901) 62.
[12] R.J. Ribando, K.E. Torrance, Natural convection in a porous medium: Effect of confinement, variable permeability, and thermal boundary condition, J. Heat Transfer (1976) 42–47.
[13] E.M. Sparrow, R.J. Goldstein, V.K. Jonsson, Thermal instability in a horizontal fluid layer: effect of boundary conditions and nonlinear temperature profile, J. Fluid Mech. 18 (1964) 513.
[14] J.W. Elder, Steady free convection in a porous medium heated from below, J. Fluid Mech. 27 (1967) 29–48.
[15] M.D. Shattuck, R.P. Behringer, G.A. Johnson, J.G. Georgiadis, Convection and flow in porous media. Part 1. Visualization by magnetic resonance imaging, J. Fluid Mech. 332 (1997) 215–245.
[16] S. Ergun, Fluid flow through packed columns, Chem. Eng. Prog. 48 (1952) 89–94.
[17] Y. Katto, T. Masuoka, Criterion for the onset of convection flow in a fluid in a porous media, J. Heat Mass Transfer 10 (1967) 297–309.
[18] J.G. Georgiadis, R.P. Behringer, M.D. Shattuck, G.A. Johnson, Interstitial velocity and temperature fields in fully saturated porous media, in: Proceedings of the 9th Symposium On Energy Sciences, US Dept. of Energy, 1991.
[19] T. Kaneko, M.F. Mohtadi, K. Aziz, An experiment study of natural convection in inclined porous media, Int. J. Heat Mass Transfer 17 (1974) 485–496.
[20] F. Chen, C.F. Chen, Experimental investigation of convective stability in a superposed fluid and porous layers when heated from below, J. Fluid Mech. 207 (1989) 311–321.
[21] J.W. Elder, Steady free convection in porous medium heated from below, J. Fluid Mech. 27 (1967) 29–48.

[22] M. Prakash, F.T. Ozden, L. Yuguo, R.T. Graham, A CFD study of natural convection heat and mass transfer in respiring hygroscopic porous media, in: Proceedings Second International Conference on CFD in the Minerals and Process Industries CSIRO, Melbourne, Australia, 1999, pp. 157–162.
[23] D.W. Stamps, V.S. Arpaci, J.A. Clark, Unsteady three-dimensional natural convection in a fluid-saturated porous medium, J. Fluid Mech. 213 (1990) 377–396.
[24] R.A. Kerr, Iceland's fires tap the heart of the planet, Science 284 (1999) 1103.
[25] O.L. Anderson, A thermal balancing act, Science 283 (1999) 1652–1654.
[26] H.S. Carslow, Jagear, Conduction of Heats in Solid, Oxford University. Press, 1973.
[27] M.A. Combarnous, S.A. Bories, Hydrothermal convection in saturated porous media, Adv. Hydrosc. 10 (1975) 231–307.
[28] J.W. Elder, Transient convection in a porous medium, J. Fluid Mech. 27 (1967) 609–623.
[29] K.Y. Tan, The simulation of heat transfer in a thermal layer, M.Sc. Thesis, Universiti Putra Malaysia, 1999.
[30] R.N. Horne, Three dimensional natural convection in confined porous media, Int. J. Heat Mass Transfer 15 (1979) 73–90.
[31] J.M. Straus, G. Schubert, Three-dimensional convection in a cubic box of fluid-saturated porous material, J. Fluid Mech. 97 (1979) 155–165.
[32] C.R.B. Lister, An explanation for multi-valued heat transport found experimentally for convection in porous medium, J. Fluid Mech. 214 (1990) 287–320.
[33] F.H. Busse, D.D. Joseph, Bounds for heat transport in a porous layer, J. Fluid Mech. 54 (1972) 521–543.
[34] B.R. Morton, On the equilibrium of a stratified layer of fluid, Quart. J. Mech. Appl. Math. 10 (1957) 433.
[35] W. Lick, The stability of a fluid layer with time-dependent heating profile, J. Fluid Mech. 21 (1965) 565.
[36] I.G. Currie, The effect of heating rate on the stability of stationary fluids, J. Fluid Mech. 29 (1967) 337.